Two-Port Dual-Band Filtering Network and Its Application on Filtering Antennas

Zhang, Yiming; Zhang, Shuai

Published in:
I E E E Antennas and Wireless Propagation Letters

DOI (link to publication from Publisher):
10.1109/LAWP.2022.3221180

Publication date:
2023

Document Version
Accepted author manuscript, peer reviewed version

Two-Port Dual-Band Filtering Network and Its Application on Filtering Antennas

Yi-Ming Zhang, *Member, IEEE*, and Shuai Zhang, *Senior Member, IEEE*

***Abstract*—This letter presents a two-port dual-band filtering network, which can be integrated with antennas for dual-band filtering antenna applications in sub-6 GHz systems. The proposed network consists of a slotline resonator and two stub groups, featuring second- and third-order resonant characteristics at the lower and upper frequencies. Analysis by establishing equivalent circuits is carried out to verify the performance of the network. Moreover, the proposed filtering network is integrated with a 2×2 antenna array. Notice that the 2×2 antenna array serves as the final resonator of the filtering network during the integration. A prototype working at 3.5 GHz and 4.9 GHz is fabricated for verification purposes. The filtering antenna array features sharp roll-off at the edges, with low insertion loss, high polarization purity, and wide fractional bandwidth of 11.7% at 3.5 GHz and 13.5 % at 4.9 GHz.**

***Index Terms*—Dual-band operation, filtering antenna, filtering power divider, slotline resonator, transmission zeros.**

I. Introduction

In order to eliminate the effect resulting from the unideal impedance matching between antennas and filters which are the two critical components for modern wireless front-end, integrations of the two components have been studied widely [1]-[13]. The main target of these investigations is to obtain filtering responses for realized gain and reflection coefficient. Seeing that excellent frequency selectivity can be achieved easily at feeding layers, one method aiming at the design of the filtering feeding network and its synthesis into antenna systems [4]-[13], is becoming popular, with a compact layout and pretty low influence on the radiation of the antennas.

Despite the numerous studies of filtering antennas, there remain some key challenges in dual-band applications [8]-[13]. According to the published reports, it is challenging for dual-band filtering antennas to achieve high-order filtering, since the out-of-band rejection between the two frequency bands and impedance bandwidth should be taken into consideration simultaneously.

In this letter, a slotline-based two-port dual-band filtering network is proposed, and a dual-band filtering antenna is further developed. Although slotline-based filtering antennas have been studied in recent years [5]-[7], these researches mainly focus on single-band operations. The scheme proposed in this letter uses a simple slotline resonator to achieve dual-band frequency selectivity, which is not mentioned or reported before. An equivalent circuit model of the proposed network is established and analyzed. Both numerical and full-wave simulated results verify the performance of the proposed filtering network. For practical demonstrations, the proposed two-port filtering network is integrated with a single-fed dual-band 2×2 patch antenna array, to realize a dual-band filtering antenna featuring a high-order filtering response (third-order at 3.5 GHz and fourth-order at 4.9 GHz).

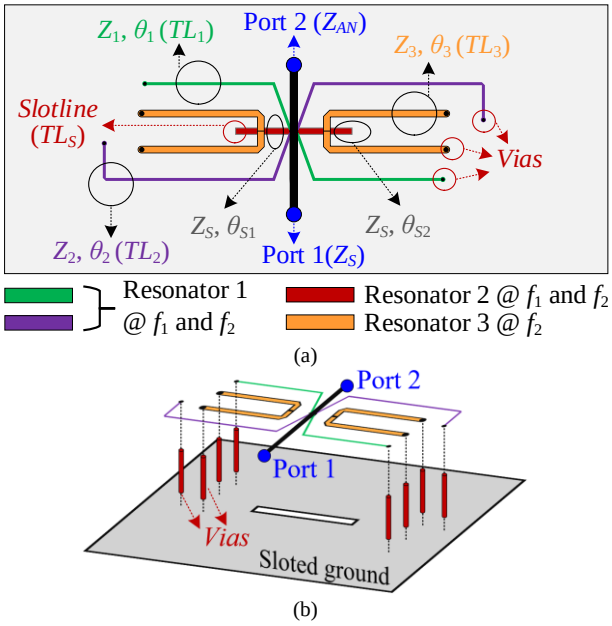

Fig. 1. Configuration of the proposed two-port dual-band filtering network. (a) Top View and (b) Three-D view.

II. Synthesis of The 2×2 Dual-Band Filtering Network

A. Synthesis of the proposed dual-band filtering network

Illustrated in Fig. 1 is the configuration of the proposed two-port filtering network. For ease of analysis, the two operating frequencies f_1 and f_2 ($f_1 < f_2$) of the dual-band scheme are set as 3.5 GHz and 4.9 GHz. Fig. 2(a) depicts the equivalent circuit model of the full configuration. Fig. 2(b) and Fig. 2(c)

This work was partially supported by Huawei project of "5G mmWave Decoupling Array". (*Corresponding author*: *Shuai Zhang*.)

Yi-Ming Zhang is with the School of Electronics and Information Technology, and Guangdong Provincial Key Laboratory of Optoelectronic Information Processing Chips and Systems, Sun Yat-Sen University, Guangzhou 510006, China. (email: zhangyim9@mail.sysu.edu.cn).

Shuai Zhang is with the Antenna, Propagation and Millimeter-wave Systems (APMS) Section, Department of Electronic Systems, Aalborg University, 9220 Aalborg, Denmark (e-mail: sz@es.aau.dk).

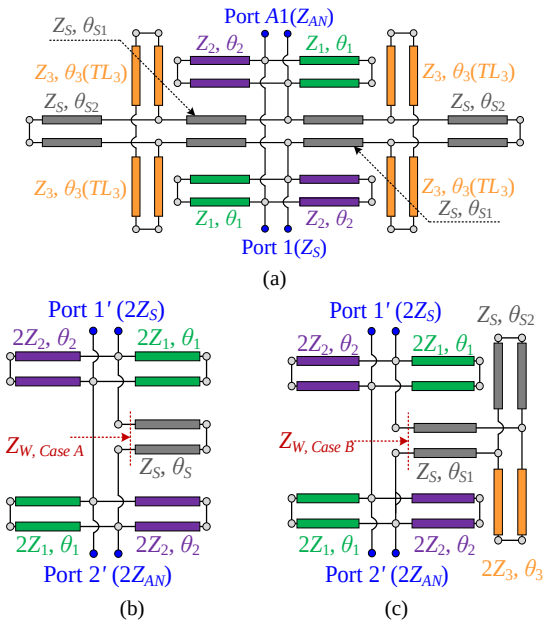

Fig. 2. Equivalent circuits of the proposed filtering network. (a) Full configuration. (b) Simplified model without the stub TL_3, marked as Case A. (c) Simplified model of the full configuration, marked as Case B.

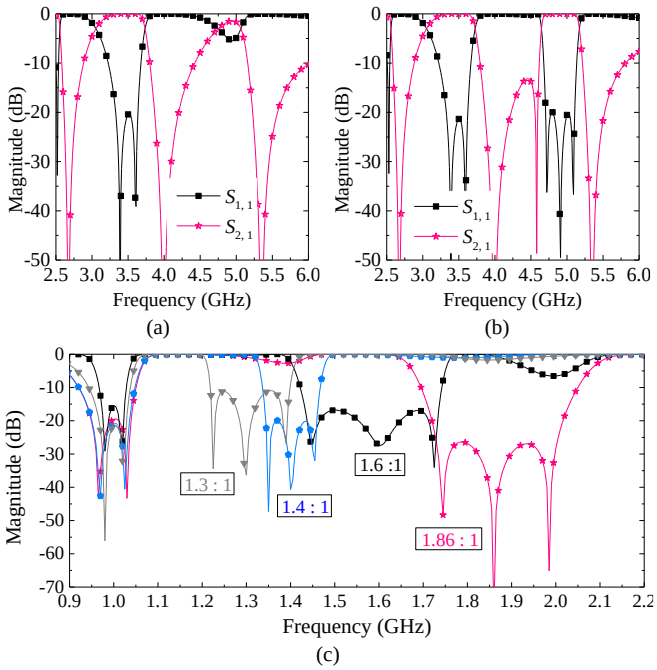

Fig. 3. Numerically calculated S parameters of the circuit models determined by the design procedure. (a) Case A. (b) Case B. (c) Different frequency ratios.

illustrate the simplified models to realize single- and dual-band responses, marked as Case A and Case B, respectively. For Case A, we have

$$\theta_S = \theta_{S1} + \theta_{S2} = \frac{\pi}{4} \tag{1}$$

The transmission responses of Case A can be calculated. It can be evaluated by network analysis that

$$S_{2,1}\big|_{Case\ A} = 0,\ if\ \ \theta_1 = \pi\ or\ \theta_2 = \pi \tag{2}$$

which implies that a transmission zero could be generated on each side of f_1 when the values of θ_1 and θ_2 depart away from 180° to the smaller or the larger ones (assuming that $\theta_1 > \pi > \theta_2$). The frequencies with the transmission zeros are determined as

$$f_{zero,1} = \frac{\pi f_1}{\theta_1},\ \ f_{zero,2} = \frac{\pi f_1}{\theta_2} \tag{3}$$

By properly selecting a group solution of Z_S, Z_1, and Z_2 once the values of θ_1 and θ_2 are given, a bandpass filtering response around the frequency f_1 can be readily achieved.

To achieve a bandpass response at f_2, two pairs of shorted stubs are loaded cross over the two ends of the slotline respectively, as shown in Case B, marked as TL_3. Note that the setting in (1) remains in Case B, and the values of θ_1, θ_2, Z_S, Z_1, and Z_2 have already been determined during the analysis of Case A. Subsequently, the transmission coefficients of Case B can be calculated. Besides, the values of $\tan\theta_1$ and $\tan\theta_2$ are nonzero and finite from f_1 to f_2 (1.4f_1), so that

$$S_{2,1}\big|_{Case\ B} = 0,\ if\ \ \theta_3 = \pi \tag{4}$$

This indicates that a transmission zero between $f_{zero,1}$ and f_2 is generated by TL_3 at the frequency $f_{zero,3}$, determined by

$$f_{zero,3} = \frac{\pi f_1}{\theta_3} \tag{5}$$

Besides, an attenuation pole can be observed at the frequency $f_{zero,4}$ based on (3), giving that

$$f_{zero,4} = 2f_{zero,1} = \frac{2\pi f_1}{\theta_1} \tag{6}$$

If we set that

$$0.5f_2 < f_{zero,1} < f_1 \tag{7}$$

there would be a transmission zero at the frequency higher than f_2. At this point, by selecting a group value of θ_{S1} and Z_3 for impedance matching purposes, a third-order bandpass response around f_2 can be obtained. Based on the derivation, all the parameter values of the dual-band filtering network can be determined.

B. *Design and analysis*

The models of Cases A and B can be determined by following the numerical analysis. Notice that f_1= 3.5 GHz, f_2 = 4.9 GHz, and $Z_S = Z_{AN}$ = 50 Ω, the S parameters of the two cases can be evaluated. The determined values are (@ f_1): θ_1 = 235.6°, θ_2 = 157.7°, θ_3 = 126.3°, θ_{S1} = 30°, θ_{S2} = 15°, Z_1 = 93 Ω, Z_2 = 93 Ω, Z_3 = 81.9 Ω, Z_S = 89.7 Ω. The calculated results are illustrated in Fig. 3. Fig. 3(a) indicates that without loading the stub TL_3 (Z_3, θ_3), a second-order bandpass response at f_1 is generated, but it is mismatched at f_2. With TL_3, second-order and third-order resonances are obtained at f_1 and f_2 respectively, as plotted in Fig. 3(b). Moreover, an additional transmission zero between f_1 and f_2 is generated to further suppress the out-of-band spurious. Notice that the frequencies of the two bands are designable based on the derivations. Fig 3(c) illustrates some results of the proposed filtering scheme with different frequency ratios. It is seen that well-designed filtering responses are achieved within the frequency ratio from 1.3 to 1.9.

C. *Integration with an antenna array*

In this part, the proposed dual-band filtering network is highly integrated with a single-fed antenna array, to realize a

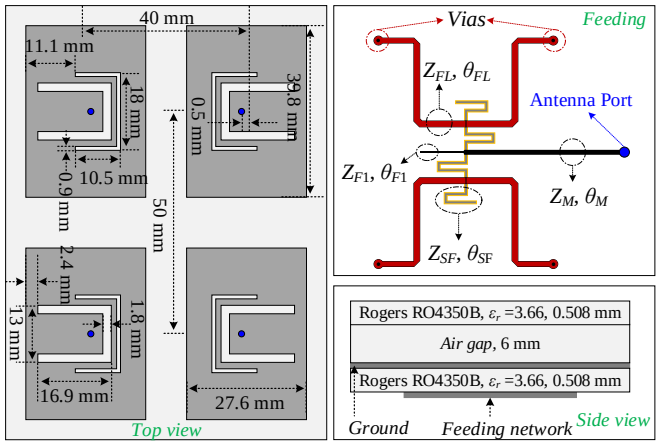

(a)

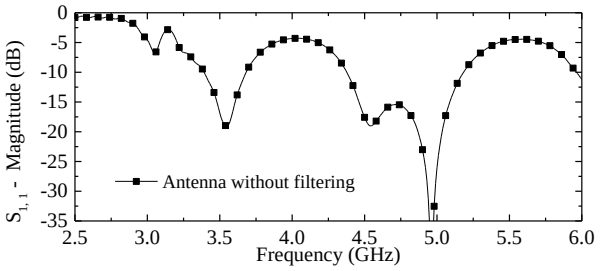

(b)

Fig. 4. Physical layout of a dual-band antenna array without filtering network, using the feeding of the basic network reported in [6]. (a) Dimensions of the 2×2 patch array. (b) *S* parameters of the single-fed antenna array.

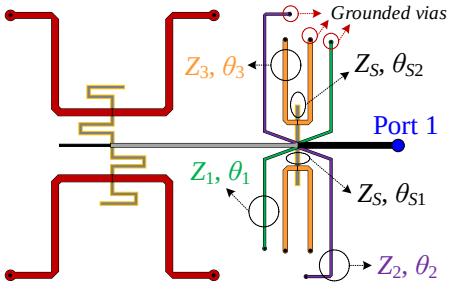

(a)

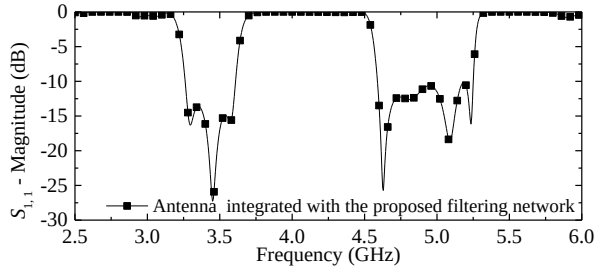

(b)

Fig. 5. (a) Configuration of the feeding integrated with the proposed filtering network. (b) Calculated *S* parameters of the dual-band 2×2 filtering antenna array integrated with the proposed filtering network.

dual-band high-order filtering antenna. The basic antenna array configuration without filtering is shown in Fig. 4(a). The antenna is a 2×2 single-fed array composed of U-slotted patch elements. The inner U-slot is utilized for dual-band operation and the outer U-slot is employed for enhancing the impedance bandwidth at the higher band. The antenna array is fed by a slotline-based four-way power splitter where a half-wavelength

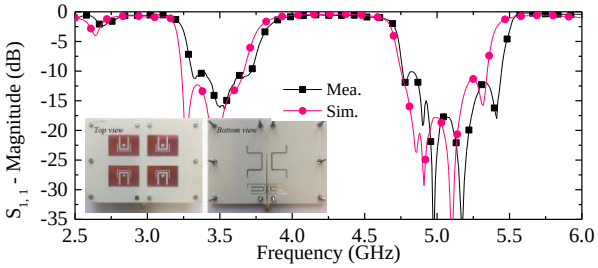

(a)

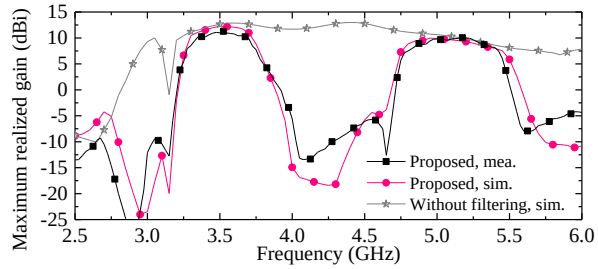

(b)

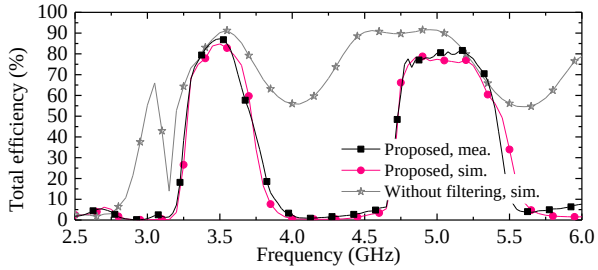

(c)

Fig. 6. Measured results of the proposed dual-band filtering antenna array. (a) *S* parameters, (c) gain and (d) total efficiency.

(referring to f_P) slotline resonator is utilized, with an insertion loss of around 0.5 dB. Note that, we use the basic configuration of the work in [6], i.e., the five-port network shown in Fig. 4(a), as a power divider without any filtering function. This indicates that no frequency selectivity is expected from the basic structure, and the dual-band filtering is contributed by the proposed two-port network. Fig. 4(b) shows the simulated S parameters of the basic antenna array, where frequency selectivity is low.

Subsequently, the proposed filtering network is integrated with the antenna array, as shown in Fig. 5(a). For ease of analysis, we set that

$$f_P = \frac{f_1 + f_2}{2} \quad \text{and} \quad \theta_{SF} = \theta_{F1} = \frac{\pi}{2}, @\ f_P \tag{8}$$

It has been discussed in [5] and [6] that antennas and filtering networks could be highly integrated by introducing an additional transition. By following the integration methods given in [5] and [6], the road impedance Z_{AN} of the antenna array involving the four-way power splitter can be derived, and the parameters Z_{SF}, Z_{F1}, Z_M, and θ_M can be determined. Based on the analysis, the four-way power divider can be established: θ_{FL} = 161.4° (@ f_1), θ_M = 218.6° (@ f_1), $\theta_{SF} = \theta_{F1}$ = 90° (@ f_P), Z_{FL} = 44.2 Ω, Z_M = 72.8 Ω, Z_{SF} = 117.4 Ω, Z_{F1} = 89.7 Ω. The calculated results of the antenna array integrated with the proposed filtlering network are provided in Fig. 5(b). The proposed array features high selectivity at the two frequency bands and sharp cut-off at the edges, as expected.

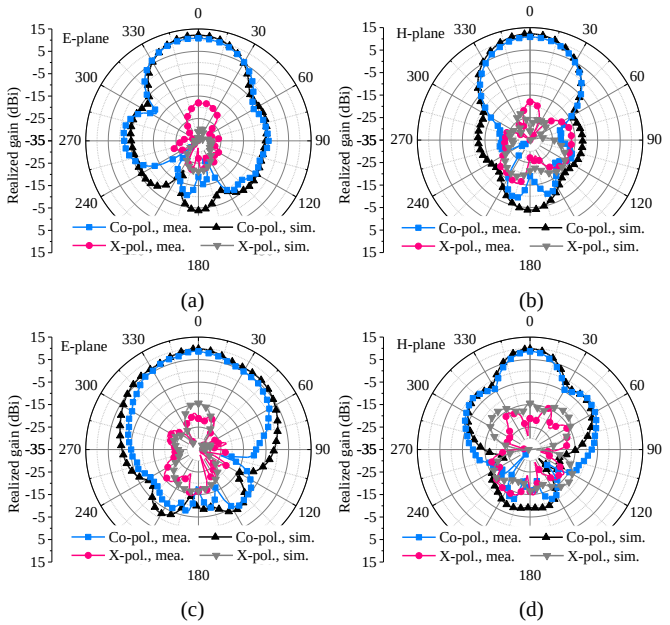

Fig. 7. Measured radiation patterns of the array. (a) E-plane at 3.5 GHz. (b) H-plane at 3.5 GHz. (c) E-plane at 4.9 GHz. (d) H-plane at 4.9 GHz.

TABLE II
COMPARISONS BETWEEN SOME RECENTLY PUBLISHED DUAL-BAND FILTERING ANTENNAS AND THE PROPOSED ONE

Ref.	Frequency (GHz) Profile (mm)	Gain (dBi) XPD (dB)	Filtering order f_L / f_H	Frequency ratio / Nulls between f_L & f_H
[8]	3.5 / 4.9 2.626	7.5 / 8.0 -40 / -30	2^{nd} / 2^{nd}	1.44 / 1
[9]	1.9 / 2.6 1.575	6.7 / 7.3 -21 / -22	2^{nd} / 2^{nd}	1.37 / 2
[10]	2.05 / 3.5 25.3	1.18 / 0 -20 / -20	2^{nd} / 2^{nd}	1.71 / 2
[11]	1.5 / 3.0 0.762	≈3.0 / ≈2.0 -20 / -20	3^{rd} / 2^{nd}	2.0 / 2
[12]	3.5 / 5.06 16.162	5.5 / 6.75 -20 / -30	1^{st} / 1^{st}	1.45 / 1
[13]	3.5 / 4.9 11.3	8.73 /9.78 -30 / -30	2^{nd} / 2^{nd}	1.4 / 1
This work	**3.5 / 4.9** **7.016**	**11.3 / 10.0** **-25 / -25**	**3^{rd} / 4^{th}**	**1.4 / 2**

III. MEASUREMENTS AND DISCUSSIONS

The design example provided in Section II-C is fabricated and assembled. Fig. 6(a) shows the measured reflection coefficient of the filtering antenna array. For comparison purposes, the result of the array without the filtering network is also provided. For the proposed array, the fractional impedance bandwidth at the two operating frequencies are 11.7% and 13.5%, respectively. The reflection coefficient within the out of band from 3.94 to 4.61 GHz is increased to high than −0.9 dB, which is lower than −4.4 dB for the referenced scheme.

As illustrated in Fig. 6(b), the maximum in-band gains of 11.3 dBi and 10.0 dBi are obtained at 3.525 GHz and 5.175 GHz, respectively. With the contribution of the transmission zeros allocated between 3.5 GHz and 4.9 GHz, the out-of-band gain is suppressed to a low level. Despite a small degradation is found compared to the referenced one, the in-band total efficiency of the proposed array is over 75%. Fig. 7 shows the radiation patterns of the array at 3.5 GHz and 4.9 GHz. The measured cross-polarization level is lower than −25 dB contributed by the differential feeding. The in-band gain is not very flat because the impedance matching performance at the resonances close to the frequency edges are not as good as the ones close to the central frequency of each band. Despite that, the gain imbalance is small and acceptable.

For comparison purposes, some published dual-band filtering antennas are summarized and listed in Table I to further describe the merits of the proposed scheme. Here, we mainly focus on the fractional bandwidth, peak gain and cross-polarization discrimination (XPD), frequency selectivity, as well as out-of-band rejection. In this work, the proposed filtering antenna features high-order in-band filtering, low cross-polarization level, simple configuration, low insertion loss, designable frequency ratio between 1.3 to 1.9. Despite an air gap being loaded, the proposed filtering antenna still keeps a low-profile level, around $0.08\lambda_L$ or $0.11\lambda_H$ (λ_L and λ_H are the free space wavelengths at the frequencies f_L and f_H, respectively). Wide-band responses are obtained with the highest peak gain. At lower and upper bands, third- and fourth-order filtering responses are achieved, respectively. Two transmission zeros in between the operating frequencies are generated facing the small frequency ratio of 1.4, leading to high frequency selectivity and good out-of-band rejection. To the best of the author's knowledge, this is the highest filtering order in dual-band filtering antenna designs around a frequency ratio of 1.4 that has been demonstrated.

IV. CONCLUSION

In this letter, a dual-band filtering network and a dual-band filtering antenna array with high frequency selectivity and wide impedance bandwidth are proposed. The presented array consists of a two-port dual-band filtering network and a single-fed dual-band patch antenna array. Firstly, the microstrip-slotline-based resonator is studied to verify the dual-band filtering response through network synthesis. Subsequently, an integration study is carried out for the patch array and the proposed network. To demonstrate the practical performance of the proposed dual-band filtering antenna array, an example is developed and measured. The proposed array features high frequency selectivity, low insertion loss, wide impedance bandwidth as well as good out-of-band rejection, making it valuable for Sub-6 GHz applications.

REFERENCES

[1] X. Yang, H. Luyen, S. Xu and N. Behdad, "Design method for low-profile, harmonic-suppressed filter-antennas using miniaturized-element frequency selective surfaces," *IEEE Antennas and Wireless Propagation Letters*, vol. 18, no. 3, pp. 427-431, March 2019.

[2] W. Yang, Y. Zhang, W. Che, M. Xun, Q. Xue, G. Shen, and W. Feng, "A simple, compact filtering patch antenna based on mode analysis with wide out-of-band suppression," *IEEE Transactions on Antennas and Propagation*, vol. 67, no. 10, pp. 6244-6253, Oct. 2019.

[3] Y. Liu, K. W. Leung, J. Ren and Y. Sun, "Linearly and circularly polarized filtering dielectric resonator antennas," *IEEE Transactions on Antennas and Propagation*, vol. 67, no. 6, pp. 3629-3640, June 2019.

[4] M. Troubat, S. Bila, M. Thevenot, D. Baillargeat, T. Monediere, S. Verdeyme, and B. Jecko, "Mutual synthesis of combined microwave

circuits applied to the design of a filter-antenna subsystem," *IEEE Transactions on Microwave Theory and Techniques*, vol. 55, no. 6, pp. 1182-1189, June 2007.

[5] Y. -M. Zhang, S. Zhang, Q.-C. Ye and G. F. Pedersen. "Cosynthesis of a filtering antenna with harmonic suppression," *IEEE Antennas Wireless Propag. Lett.,* vol. 19, no. 10, pp. 1729-1733, Oct. 2020.

[6] Y. -M. Zhang, S. Zhang, G. Yang and G. F. Pedersen, "A wideband filtering antenna array with harmonic suppression," *IEEE Trans. Microw. Theory Techn.*, vol. 68, no. 10, pp. 4327-4339, Oct. 2020.

[7] S. Ji, Y. Dong and Y. Fan, "Bandpass filter prototype inspired filtering patch antenna/array," *IEEE Trans. Antennas Propag.*, vol. 70, no. 5, pp. 3297-3307, May 2022.

[8] C. X. Mao, S. Gao, Y. Wang, B. S.-Izquierdo, Z. Wang, F. Qin, Q. X. Chu, J. Li, G. Wei, and J. Xu, "Dual-band patch antenna with filtering performance and harmonic suppression," *IEEE Trans. Antennas Propag.*, vol. 64, no. 9, pp. 4074-4077, Sept. 2016.

[9] X. Y. Zhang, Y. Zhang, Y. Pan and W. Duan, "Low-profile dual-band filtering patch antenna and its application to LTE MIMO system," *IEEE Trans. Antennas Propag.*, vol. 65, no. 1, pp. 103-113, Jan. 2017.

[10] P. F. Hu, Y. M. Pan, K. W. Leung and X. Y. Zhang, "Wide-/dual-band omnidirectional filtering dielectric resonator antennas," *IEEE Trans. Antennas Propag.*, vol. 66, no. 5, pp. 2622-2627, May 2018.

[11] W. Xie, J. Wang, W. Wang, Y. Wu and Y. Liu, "Wideband/dual-band reconfigurable filtering antenna for wireless communication systems," *2019 IEEE MTT-S International Wireless Symposium (IWS)*, Guangzhou, China, 2019, pp. 1-3.

[12] C. Wang, Z. Han, H. Liu, X. Zhang and L. Wang, "A dual-band filtering dielectric resonator antenna," *2020 9th Asia-Pacific Conference on Antennas and Propagation (APCAP)*, Xiamen, China, 2020, pp. 1-2.

[13] Y. Li, Z. Zhao, Z. Tang and Y. Yin, "Differentially fed, dual-band dual-polarized filtering antenna with high selectivity for 5G sub-6 GHz base station applications," *IEEE Trans. Antennas Propag.*, vol. 68, no. 4, pp. 3231-3236, April 2020.